Materials Research Bulletin 51 (2014) 426–431

Contents lists available at ScienceDirect

Materials Research Bulletin

journal homepage: www.elsevier.com/locate/matresbu

Comparative study of microstructure, electric properties and conductivity for NiO and PNN modified $Pb(Zn_{1/3}Nb_{2/3})O_3$–$PbZrO_3$–$PbTiO_3$ ceramics

Mupeng Zheng, Yudong Hou *, Mankang Zhu, Ming Zhang, Hui Yan

College of Materials Science and Engineering, Beijing University of Technology, Beijing 100124, China

ARTICLE INFO

Article history:
Received 6 October 2013
Received in revised form 4 December 2013
Accepted 30 December 2013
Available online 8 January 2014

Keywords:
A. Ceramics
D. Microstructure
D. Dielectric properties
D. Ferroelectricity

ABSTRACT

The comparative studies of NiO and $Pb(Ni_{1/3}Nb_{2/3})O_3$ (PNN) added $Pb(Zn_{1/3}Nb_{2/3})O_3$–$PbZrO_3$–$PbTiO_3$ (PZN–PZT) with the same content level of Ni ions have been performed. On the basis of the XRD and TEM analysis, it is clear that NiO introduction induces a phase transformation from the morphotropic phase boundary (MPB) to the tetragonal phase side, and the corresponding grain size increases greatly. In comparison, the system with PNN addition remains MPB structure, and the corresponding grain size increases slightly. According to the analysis of temperature dependencies of dielectric constant and AC conductivity, combined with the observed evolution trend of ferroelectric loops, it is reasonable to deduce that two types of substitution behaviors coexist in NiO added PZN–PZT system. The doping Ni^{2+} ions can not only substitute for Ti^{4+}, Zr^{4+} and Nb^{5+} ions in the inequivalence replacement, but also substitute for Zn^{2+} ions in the equivalence replacement.

1. Introduction

Solid solutions between a normal ferroelectric $Pb(Zr,Ti)O_3$ (PZT) and a relaxor ferroelectric $Pb(Zn_{1/3}Nb_{2/3})O_3$ (PZN), namely PZN–PZT ceramics, have been intensively studied recently due to their excellent electrical performance, which shows possible application to actuators, transducers and piezoelectric ultrasonic motors [1–3]. As is well known, many macroscopic physical properties of piezoelectric ceramics such as piezoelectric coefficients (d_{33}), electromechanical coupling factors (k_p), dielectric constant (ε_r), and dielectric loss ($\tan\delta$), depend strongly on the ferroelectric domain structures and domain wall motion, which can be tailored to a wide extent by introducing various additives to the PZT matrix [4–6]. There is a long standing question about the mechanism of contributions from additives in PZT ceramics. With only 1–2% additives adding, the piezoelectric properties can be improved greatly even doubled. Recently, Li et al. [7] have found that when large amounts of aliovalent doping cations are present or when there are substantial amount of charged defects in the system, charged domain walls can produce much larger contribution to functional properties than charge neutral domain walls because they are energetically less stable. However, the effect of additives is a complex matter and there still exists the contradiction in the doping mechanism reported in different literatures. Previous studies have investigated the effect of transition metal oxide (Cr_2O_3, MnO_2, and Fe_2O_3) on microstructure and piezoelectric properties of PZN–PZT ceramics [8–10]. It is suggested that the introduced doping cations with relative low valence prefer to enter into the *B* sites of the perovskite lattice to substitute for Zr^{4+} and Ti^{4+} ions, which facilitates the formation of oxygen vacancy due to the charge compensation effect. This explanation is a widely accepted "acceptor" doping mechanism originated from the classic doping theory in PZT. However, it should be noted that for the PZN–PZT ternary system, the incorporation of PZN relaxor to PZT will introduce additional Zn^{2+} and Nb^{5+} ions to the *B*-site except for the host Zr^{4+} and Ti^{4+} ions, which makes the perovskite structure more complicated and enhances the difficulty in analyzing the substitution mechanism. Recently, Yan et al. [11] have investigated substitution behaviors of MnO_2 in PZN–PZT matrix. Combined X-ray diffraction analysis with energy dispersive spectroscopy, they proposed a new doping mechanism that the introduced Mn^{2+} ions can substitute for Zn^{2+} ions in the equivalence replacement. Yan et al. attributed this phenomenon to the good phase stability of $Pb(Mn_{1/3}Nb_{2/3})O_3$ (PMnN) compared to that of PZN, and the formation of PMnN favors to stabilize the perovskite phase in the ceramic processing. This new view has provoked considerable interest into such substitution behavior in the complex ternary PZN–PZT based system. Hence, although doped PZN–PZT based ceramics have been explored for many years, the doping mechanism remains debatable, and more substantial supporting

* Corresponding author. Tel.: +86 10 67392445; fax: +86 10 67392445.
E-mail address: ydhou@bjut.edu.cn (Y. Hou).

0025-5408/$ – see front matter © 2014 Elsevier Ltd. All rights reserved.
http://dx.doi.org/10.1016/j.materresbull.2013.12.061

evidences are urgently needed to give a full explanation on the substitution behaviors.

In this article, as an extension to the research on doping behaviors, NiO were selected as representatives of dopants to modulate the microstructure and the electrical properties of the PZN–PZT system. Considering the relatively high stability of $Pb(Ni_{1/3}Nb_{2/3})O_3$ (PNN) compared to that of PZN [12], it is speculated that the substitution of Ni^{2+} for host Zn^{2+} ions in the equivalence replacement would occur according to Yan's view. In order to thoroughly clarify the doping mechanism, the comparative studies of microstructure, conductivity, dielectric and ferroelectric behaviors of PZN–PZT, NiO-modified PZN–PZT and PNN–PZN–PZT has been conducted. Emphasis was placed on the influence of lattice occupation behavior of Ni cations on phase transition, domain structure evolution, grain boundary configuration and the electrical response within the samples.

2. Experimental procedure

Three compositions, (1) $0.2Pb(Zn_{1/3}Nb_{2/3})O_3$–$0.4PbZrO_3$–$0.4PbTiO_3$ (PZN–PZT), (2) 4 mol% NiO-doped $0.2Pb(Zn_{1/3}Nb_{2/3})O_3$–$0.4PbZrO_3$–$0.4PbTiO_3$ (PZN–PZT + NiO), and (3) $0.12Pb(Ni_{1/3}Nb_{2/3})O_3$–$0.08Pb(Zn_{1/3}Nb_{2/3})O_3$–$0.4PbZrO_3$–$0.4PbTiO_3$ (PNN–PZN–PZT, with the equal content of Ni ions to PZN–PZT + NiO), were synthesized by conventional mixed-oxide reaction. Reagent-grade oxide powders, Pb_3O_4, ZrO_2, TiO_2, ZnO, Nb_2O_5, and NiO were used as starting materials. The powders were weighed according to stoichiometric ratio and mixed through ball milling, with partially stabilized zirconia balls as media, in alcohol for 24 h. After drying, the mixture was calcined in a covered alumina crucible at 850 °C for 2 h. The calcined powders were remilled for 24 h and then pressed into disks of 11.5 mm in diameter at around 100 MPa. The green disks were sintered at 1050 °C for 2 h in a sealed alumina crucible. To minimize PbO loss, a PbO-rich atmosphere was maintained by placing powders of $PbZrO_3$ inside the crucible used as packing powders. The high relative densities above 97% were achieved for all specimens determined by the Archimedes technique.

The crystal structures of the samples were examined by XRD (Bruker D8 Advance, Germany) in the $\theta - 2\theta$ configuration using Cu Kα radiation. Micromorphology was detected on a thermally etched surface by SEM (Hitachi S4800, Japan) and the mean grain size was calculated by the line intercept method. TEM was carried out using an instrument (Hitachi FEI Tecnai F20, USA) operated at an accelerating voltage of 200 kV. Specimens for the TEM studies were prepared by the standard procedure of mechanical thinning, dimpling, and ion milling toward electron transparency before TEM observation. Ar^+ ion beam milling was applied to prepare the specimens by using a 5 kV potential combined with a gun current of 2.2 mA at an incidence angle of 15° to the rotating sample.

To measure the electrical properties, pellets were prepared by polishing the surface, applying a low-temperature silver paste (BQ5177, Uninwell) to the parallel plane faces and firing at 560 °C for 30 min to remove the organics form. The dielectric property and its dependence on temperature were measured using a multi-frequency inductance capacitance resistance (LCR) analyzer (Agilent E4980A, Santa Clara, CA) with an automated temperature controller. Ferroelectric behavior was studied using a ferroelectric tester (Premier II, Radiant Technologies Inc., Albuquerque, NM) at 1 Hz. The electric field-induced strain (*S*-*E*) measurements were carried out using a linear variable fiber-optic transducer (MTI 2000 Fotonic Sensor). AC conductivity measurement was conducted using impedance analyzer (Novocontrol Technologies, Germany) in the frequency range from 1 mHz to 10 MHz and temperature range between 280 °C and 360 °C.

3. Results and discussion

3.1. Microstructure and phase transition

The X-ray diffraction analysis of the sintered PZN–PZT, PZN–PZT + NiO and PNN–PZN–PZT ceramics are shown in Fig. 1(a). All specimens show a complete perovskite structure without detectable traces of the pyrochlore or other impurities. As we known, the piezoelectric performance of PZT-based ceramics are especially sensitive to the perovskite phase structure, which can be quantified by assessing relative intensities of (0 0 2) and (2 0 0) peaks. To determine the phase evolution, fine scanning was carried out in the diffraction angle range of $2\theta = 43$–$46°$, and the results are shown in Fig. 1(b). The diffraction peaks were separated by fitting the Gaussian–Lorentz line shape, and the positions of the reflections were fixed using the least square method. In general, the reflections at 45° can be divided into three peaks corresponding to tetragonal (0 0 2), rhombohedral (2 0 0), and tetragonal (2 0 0), respectively. To quantitatively investigate the effect of NiO addition on phase transformation, the tetragonal phase content (*T.P.*) was calculated using Eq. (1):

$$T.P.\ (\%) = \frac{I_{(200)T} + I_{(002)T}}{I_{(200)T} + I_{(002)T} + I_{(200)R}} \times 100 \quad (1)$$

where $I_{(2\,0\,0)R}$ is the integral intensity of rhombohedral (2 0 0) reflection, and $I_{(0\,0\,2)T}$ and $I_{(2\,0\,0)T}$ are the integral intensities of tetragonal (0 0 2) and (2 0 0) reflections, respectively [13]. The results of the calculation using Eq. (1) are shown in Fig. 1(b). For the PZN–PZT and PNN–PZN–PZT specimens, the content of the tetragonal phases are approximately 56% and 58%, and very close amounts of rhombohedral and tetragonal phases imply the presence of MPB [14]. While for the PZN–PZT + NiO composition, the content of the tetragonal phases are increased to approximately 70%, which reveals the obvious phase transition from MPB to tetragonal side.

Microstructure analysis at the nanoscale further corroborated above phase transition analysis. Typical domain structures of PZN–PZT and PZN–PZT + NiO samples are revealed by TEM studies, as depicted in Fig. 2(a) and (b). Based on the classic view of the domain theory [6], rhombohedral PZT has polarization vectors that intersect the domain walls at 71° and 109°, giving walls lying on the $\{1\,1\,0\}_p$ and $\{1\,0\,0\}_p$ planes, whereas the polarization vectors in the tetragonal PZT intersect the domain wall at 90°, giving domain walls lying on the $\{1\,1\,0\}_p$ plane. Due to the co-existence of rhombohedral and tetragonal phase in the prepared PZN–PZT ceramic, both the lamellar tetragonal domains and the lenticular

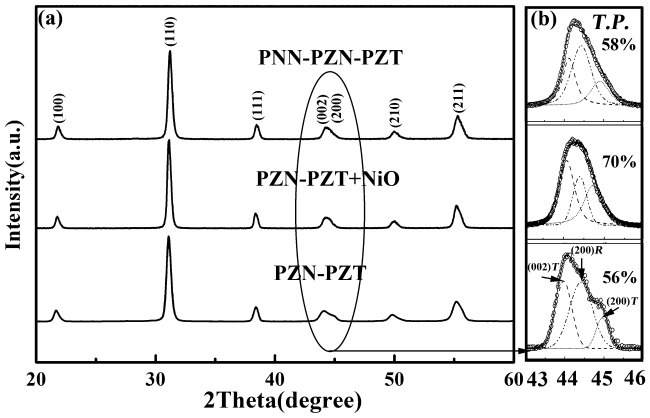

Fig. 1. (a) XRD patterns and (b) comparison of $(0\,0\,2)T$, $(2\,0\,0)R$, and $(2\,0\,0)T$ reflections (from left to right) for PZN–PZT, PZN–PZT + NiO, and PNN–PZN–PZT sintered samples.